JOC Article

Structure, Conformation, Stereodynamics, Dimer Formation, and Absolute Configuration of Axially Chiral Atropisomers of Hindered Biphenyl Carbinols

Daniele Casarini,[†] Lodovico Lunazzi,[‡] Michele Mancinelli,[‡,1] Andrea Mazzanti,*[,‡] and Carlo Rosini[†]

Department of Organic Chemistry "A. Mangini", University of Bologna, Viale Risorgimento 4, Bologna 40136, Italy, and Department of Chemistry, University of Basilicata, via N. Sauro 85, Potenza 85100, Italy

mazzand@ms.fci.unibo.it

Received July 9, 2007

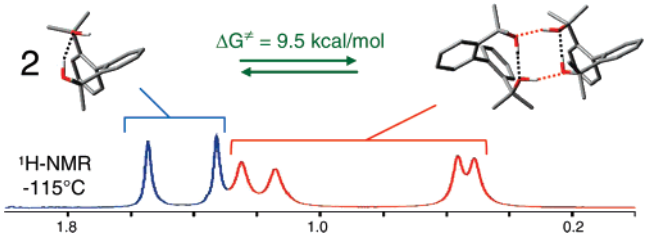

NMR spectra of biphenyl derivatives bearing a single CR_2OH substituent in the ortho position indicate that they exist as sp (more stable) and ap (less stable) conformers, due to the restricted rotation about the Ar−CR_2OH bond. When R = Et (compound **2**) the corresponding rotation barrier was determined (7.5 kcal mol^{-1}) by line shape simulation of the low-temperature NMR spectra. Introduction of the prochiral *i*-Pr group in the position 3′ of a biphenyl with the CMe_2OH substituent in the position 2 (**4**) allowed the determination of the enantiomerization barrier (due to the Ar−Ar bond rotation) for the stereolabile axially chiral atropisomers (13.9_5 kcal mol^{-1}). DFT computations of these barriers were all in agreement with the experiments. Biphenyls bearing two CR_2OH groups in the 2,2′ positions were found to exist as configurationally stable atropisomers: when R = Me (**7**) they were separated by enantioselective HPLC and the absolute configuration assigned on the basis of the corresponding CD spectra. In solution, compounds **6** (R = H) and **7** (R = Me) were found to originate a dimer, due to H-bond interactions between two enantiomers. In the case of **7**, the free energy of activation (9.5 kcal mol^{-1}) for the exchange of the monomer with the dimer could be measured, for the first time, by dynamic NMR. The conformational preferences, predicted by computations for the biphenyls with two CR_2OH substituents in the 2,2′ positions, were confirmed by X-ray diffraction in the case of R = H (**6**), R = Me (**7**), and R = *i*-Pr (**9**).

Introduction

Enantiomerism generated by axial chirality has been receiving increasing attention, as reported in a recent comprehensive review by Bringmann at al.[2] This is because structures having a biaryl axis represent the basis for reagents or catalysts employed in the asymmetric synthesis.[2] Biphenyl derivatives exhibiting axial chirality can be either configurationally stable or can give raise to stereolabile atropisomers, depending on the extent of the steric effects of their substituents. Dynamic NMR spectroscopy has been used as an efficient tool to investigate conformational enantiomers generated by axial chirality due to restricted Ar−Ar bond rotation.[3,4] We have also investigated in the recent past stereolabile atropisomerism arising from restricted rotation about the sp^2−sp^3 bond in a number of hindered aryl carbinols and ethers.[5]

[†] University of Basilicata.
[‡] University of Bologna.
(1) In partial fulfillment for a Ph.D. in Chemical Sciences, University of Bologna.
(2) Bringmann, G.; Price Mortimer, A. J.; Keller, P. A.; Gresser, M. J.; Garner, J.; Breuning, M. *Angew. Chem., Int. Ed.* **2005**, *44*, 5384 and references quoted therein.
(3) Bott, G.; Field, L. D.; Sternhell, S. *J. Am. Chem. Soc.* **1980**, *102*, 5618.
(4) (a) Lunazzi, L.; Mazzanti, A.; Minzoni, M.; Anderson, J. E. *Org. Lett.* **2005**, *7*, 1291. (b) Mazzanti, A.; Lunazzi, L.; Minzoni, M.; Anderson, J. E. *J. Org. Chem.* **2006**, *71*, 5474. (c) Lunazzi, L.; Mazzanti, A.; Minzoni, M. *J. Org. Chem.* **2006**, *71*, 9297.

10.1021/jo701481m CCC: $37.00
Published on Web 08/31/2007

CHART 1

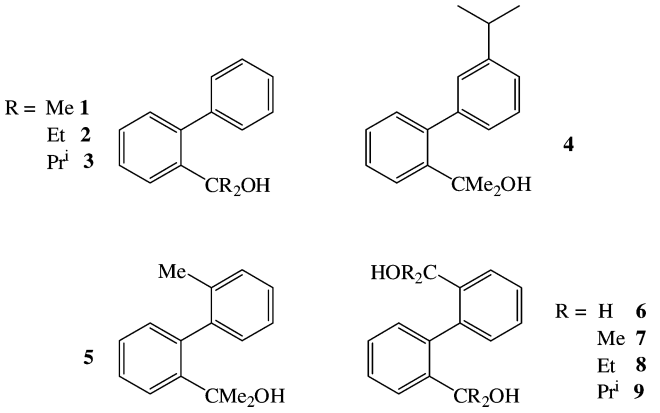

SCHEME 1

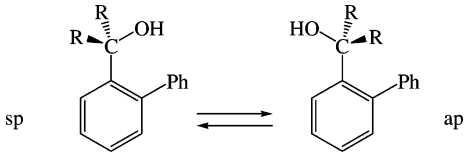

It was thus attractive to study the atropisomerism occurring in derivatives bearing both a sp^2-sp^2 and a sp^2-sp^3 chiral axis, i.e., biphenyls substituted by one or two carbinol moieties, as those displayed in Chart 1.

Results and Discussion

Dynamic NMR. Contrary to the case of analogously hindered ortho-substituted benzylcarbinols,[5b] the low temperature (down to −170 °C) NMR spectra of **1** (R = Me) do not exhibit the two groups of signals expected for the two possible conformers displayed in Scheme 1 (antiperiplanar and synperiplanar).[6] DFT calculations[7] suggest that the relative stability of the two conformational isomers is the result of a delicate balance between the steric hindrance exerted by the two aliphatic groups on the phenyl ring in the ortho position and the possibility of an energy stabilization due the position of the some hydrogen atoms over the π-system of the orthogonal phenyl ring. In the case of compound **1**, calculations indicate that both conformers[8] correspond to energy minima and should have essentially the same stability (see Figure S1, Supporting Information). However, the barrier calculated for the interconversion occurring via the Ar−CMe$_2$ bond rotation is predicted to be quite low (about 5 kcal mol^{-1}), thus accounting for the failure to detect separate NMR signals for the two conformers at any attainable temperature. The presence of both the syn and anti conformers in rapid equilibrium is also demonstrated by NOE experiments. As shown in Figure S2 (Supporting Information), irradiation of the OH signal of **1** enhances that of the single aromatic hydrogen in position ortho[9] to the CMe$_2$OH moiety, indicating the presence of the anti (ap) conformer, as well as that of the two ortho hydrogens[9] within the unsubstituted phenyl ring, indicating the presence of the syn[8] conformer.

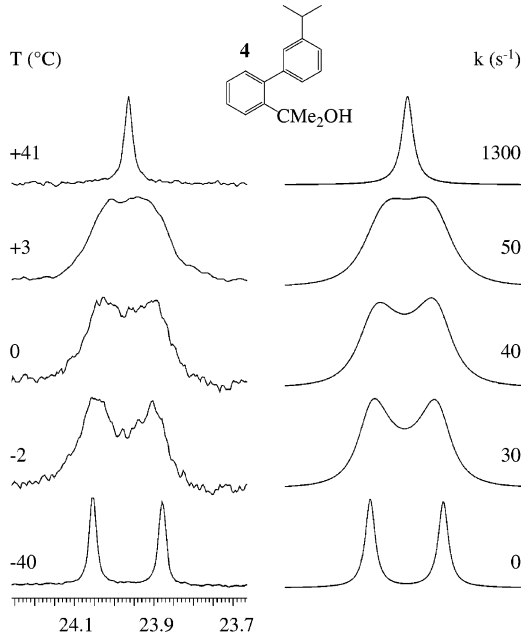

FIGURE 1. Temperature dependence of the ^{13}C (150.8 MHz) of the isopropyl methyl signals of **4** in $CDCl_3$ (left). Simulation obtained with the rate constants indicated (right).

DFT computations[7] also predict that the Ar−Ar rotation barrier of **1** should be relatively high (14.5 kcal mol^{-1}), but this motion is NMR invisible in **1** owing to the molecular symmetry. In order to detect experimentally such a process an isopropyl group was introduced in the meta position of the unsubstituted phenyl ring, yielding compound **4**: the substitution in this position, in fact, should not affect significantly the value of the Ar−Ar rotation barrier. At −40 °C, the ^{13}C methyl signals of both the isopropyl (Figure 1) and CMe$_2$OH moieties of **3** split into 1:1 pairs. This proves that the Ar−Ar rotation rate has become slow in the NMR time scale and that the molecule has adopted an asymmetric (C_1 point group) conformation where the two aryl groups are nearly orthogonal to each other. The low temperature observation of anisochronous signals for these diastereotopic methyl groups[10] implies the presence of two stereolabile atropisomers due to the chirality axis: the corresponding enantiomerization barrier, brought about by the Ar−Ar rotation, was determined by line shape simulation (Figure 1). The resulting value of $13.9_5 \pm 0.15$ kcal mol^{-1} (Table 1) is indeed very close to that anticipated by calculations (14.7 kcal mol^{-1}).

The greater steric hindrance occurring in compound **2** (R = Et) with respect to **1** allowed the detection of separate NMR signals for the corresponding sp and ap conformers. In Figure 2, the ^{13}C lines of two aromatic quaternary carbons are displayed as a function of temperature: the ratio of the two atropisomers appears to be 70:30. Computations predict that the relative energies of the two isolated sp and ap atropisomers are

(5) (a) Casarini, D.; Lunazzi, L.; Mazzanti, A. *J. Org. Chem.* **1997**, *62*, 3315. (b) Casarini, D.; Coluccini, C.; Lunazzi, L.; Mazzanti, A. *J. Org. Chem.* **2005**, *70*, 5098. (c) Casarini, D.; Coluccini, C.; Lunazzi, L.; Mazzanti, A. *J. Org. Chem.* **2006**, *71*, 4490.

(6) Eliel, L. E.; Wilen, S. H. *Stereochemistry of Organic Compounds*; J. Wiley and Sons: New York, 1994: p 21.

(7) Program Gaussian 03, Revision D.01, Frisch, M. J. et al. Gaussian, Inc., Wallingford CT, 2004 (see the Supporting Information).

(8) In the case of **1**, the syn structure might be rather called synclinal (sc): according to computations, in fact, the corresponding O−C(Me2)−C1−C2 diehdral angle (47°) exceeds 30°.[6]

(9) Assignment obtained by means of the COSY bidimensional sequence.

(10) (a) Mislow, K.; Raban, M. *Top. Stereochem.* **1967**, *1*, 1. (b) Jennings, W. B. *Chem. Rev.* **1975**, *75*, 307. (c) Eliel, E. L. *J. Chem. Educ.* **1980**, *57*, 52. (d) Casarini, D.; Lunazzi, L.; Macciantelli, D. *J. Chem. Soc., Perkin Trans.* **1992**, *2*, 1363.

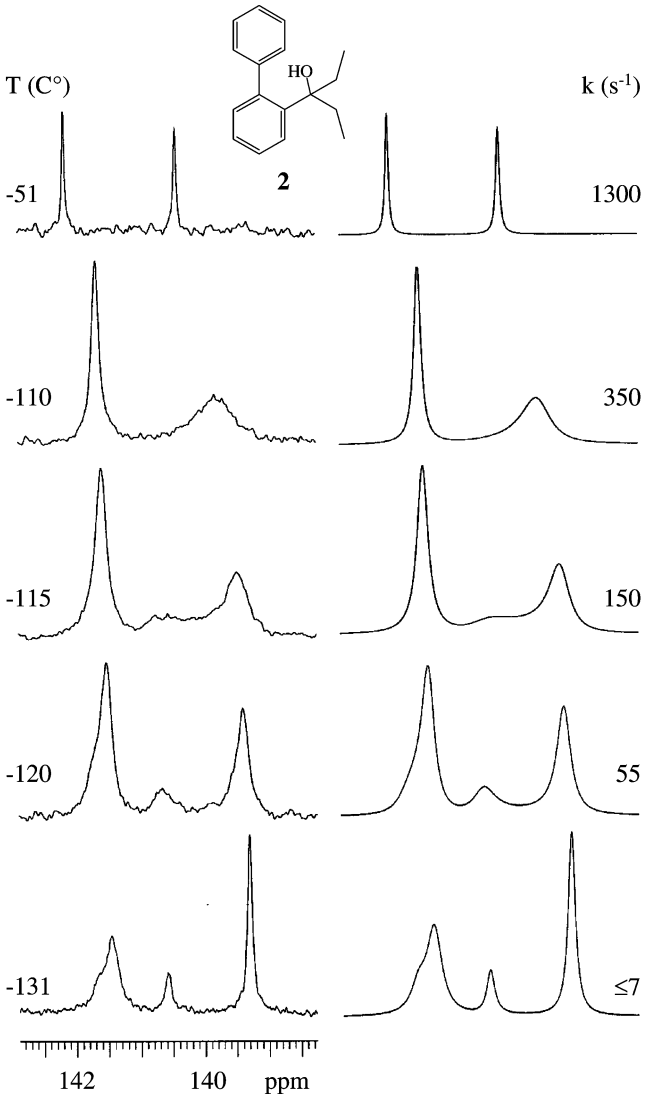

FIGURE 2. Temperature dependence of the ^{13}C NMR signals (150.8 MHz) of the lines of two aromatic quaternary carbons of **2** in $CHF_2Cl/CHFCl_2$ (left). Simulation obtained with the rate constants indicated (right).

TABLE 1. Barriers for the Dynamic Processes Measured in 2−4 and 7

compd	$\Delta G^{\ddagger}$ (kcal mol^{-1})	dynamic process
2	7.5 ± 0.15	Ph−CEt_2OH rotation
3	6.4 ± 0.15	Me_2CH−C(OH)Ar rotation
4	$13.9_5 \pm 0.15$	Ar−Ar rotation
7	9.5 ± 0.3	dimerization

essentially equal (Figure S1, Supporting Information); thus the unequal proportion observed should be attributed to the effect of the condensed phase. Nonetheless, the ap structure has been assigned to the more populated of the two conformers on the basis of the chemical shift predicted by DFT computations. In fact, the aromatic quaternary carbon ortho to the CEt_2OH moiety,[11] the aliphatic quaternary carbon, and the CH_2 carbon are all predicted to have shifts at higher field in the ap with respect to the corresponding carbons of the sp conformer.[12] In all these cases, the experimental spectrum shows that the upfield is more intense than the downfield ^{13}C signal (see Figure 2 and Figure S3, Supporting Information).

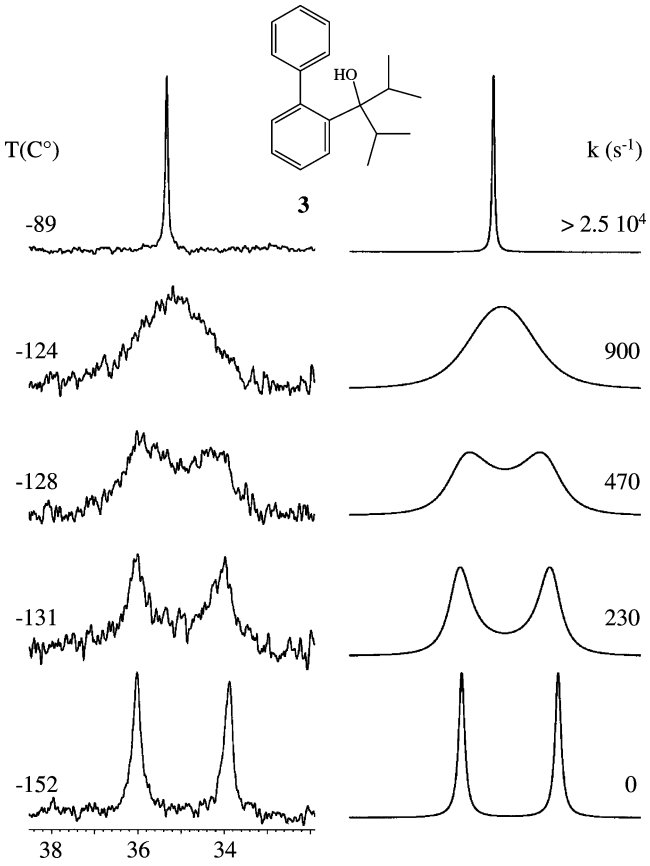

FIGURE 3. Temperature dependence of the CH isopropyl signal of **3** (^{13}C NMR at 150.8 MHz) in $CHF_2Cl/CHFCl_2$ (left). Simulation obtained with the rate constants indicated (right).

From the line shape simulation of the spectrum of Figure 2 the barrier for the interconversion of the major (ap) into the minor (sp) conformer is derived (7.5 ± 0.15 kcal mol^{-1}, as in Table 1): the same value was also obtained by simulating the ^{13}C signals of the CH_2 carbon (Figure S3, Supporting Information).

Although the greater steric requirements of **3** (R = *i*-Pr) would suggest a barrier for the interconversion larger than that of **2** (R = Et), the corresponding ^{13}C NMR spectrum does not show the two expected sets of unequally intense signals, even at −152 °C. This means that in the case of **3** only one of the two possible conformers is appreciably populated.

Calculations actually show that the sp form has an energy 3.2 kcal mol^{-1} lower than that of its ap companion, thus accounting for the negligible population of the latter. The structure computed for the more stable sp conformer of **3** indicates that the two isopropyl groups are locked in two different spatial situations (Figure S1, Supporting Information) since they exhibit two different values (58° and 170°) for the H−C(Me_2)−C(OH)-C_{ipso} dihedral angles. Indeed, the ^{13}C spectrum of **3** at −152 °C displays two equally intense signals for the two isopropyl CH carbons (Figure 3), and in addition, also one of the two lines, due to the two pairs of methyl carbons

(11) Assignment obtained by means of the HMBC bidimensional sequence.

(12) The computed differences between the shifts of these carbons are 1.1, 1.5, and 1.4 ppm, to be compared with the corresponding experimental differences (measured at −131 °C) of 1.26, 2.56, and 1.70 ppm, respectively. The other carbons either have shift differences too small to be significant or are overlapped by the signals of the solvent ($CHF_2Cl/CHFCl_2$).

(that are already diastereotopic at ambient temperature[10]), is further split into 1:1 lines at −152 °C (the additional splitting, expected for the other diastereotopic methyl line, had a shift difference too small to be detected). The line shape simulation of the signals of Figure 3 yields a barrier of 6.5 kcal mol^{-1} for the rotation process of the isopropyl substituents about the HOC−CHMe$_2$ bond (the same barrier was also obtained by simulating the corresponding ^{1}H signals, as in Figure S4, Supporting Information): this value is in keeping with that (6.4 kcal mol^{-1}) determined in an analogous case.[5b]

The presence of an *o*-methyl substituent in the phenyl moiety of compound **5** enhances the Ar−Ar rotation barrier and, at the same time, renders the molecule asymmetric since the two aryl rings adopt an orthogonal arrangement, as anticipated by calculations (Supporting Information). For this reason, the ambient temperature NMR spectrum of **5** displays two anisochronous lines for the methyl groups because they have been made diastereotopic[10] by the chirality of the molecule. Even at higher temperature (+120 °C in DMSO-d_6), these lines do not undergo an exchange process, indicating that the Ar−Ar rotation barrier, required to interconvert the two enantiomers, is, at least, higher than 21−22 kcal mol^{-1} (DFT computations predict a barrier of 25.1 kcal mol^{-1}). As already observed in the case of compounds **1** and **4**, low temperature spectra (Figure S5, Supporting Information) do not show any dynamic feature due to slow rotation of the C−Me$_2$OH moiety.

In the case of biphenyls bearing two equal CR$_2$OH substituents in the ortho and ortho′ positions (Chart 1), the Ar−Ar rotation barrier is likewise quite high, so that two relatively stable atropisomers are expected to occur. For instance, derivative **6** (R = H) displays at ambient temperature an AB-type spectrum for the diastereotopic methylene hydrogens of the CH$_2$OH moiety[13] (Figure 4, top): even on warming above ambient temperature this diastereotopicity is maintained.

The three conformers corresponding to the lowest energy minima computed[7] for **6** and **7** are displayed in Scheme 2. As conceivable, the computed Ar−CH$_2$OH rotation barrier, required to interconvert these conformers, is so low (less than 4 kcal mol^{-1}) as to be NMR invisible at any attainable temperature. The computed minimum of energy corresponding to the sp,ac is much lower than for the other two structures (i.e., sp,sp and ap,ap); thus, derivative **6** is expected to adopt essentially this conformation.

On lowering the temperature, the spectral lines of **6** broaden and, subsequently, sharpen again, in a way typical of an exchange process (Figure 4). Since, as mentioned, the barrier to freeze the Ar−CH$_2$OH rotation is NMR invisible, the observed dynamic process was attributed to the exchange of the sp,ac monomer with a dimer, assembled by two intermolecular H-bond interactions between the pairs of the OH groups of two sp,ac conformers.

DFT calculations[7] indicate, in fact, that a heterochiral dimer, formed by an M and a P enantiomer of the sp,ac conformer, corresponds to a minimum, with an energy value much lower than that of the homochiral dimer formed by two M (or two P) enantiomers (Figure S6, Supporting Information): thus, only the heterochiral dimer (meso) should be present, whereas the M,M (or P,P) homochiral dimer (racemic) should not be populated. The static symmetry of the dimer of **6** (Figure S6, Supporting Information) is C_i, but the rapid rotation about the C−OH bonds in this meso structure makes the dynamic symmetry higher, thus rendering equivalent (i.e., isochronous) the shifts (both ^{13}C and ^{1}H) of the four CH$_2$OH moieties of the dimer. Within each CH$_2$OH moiety, however, the two methylene hydrogens would always remain diastereotopic.

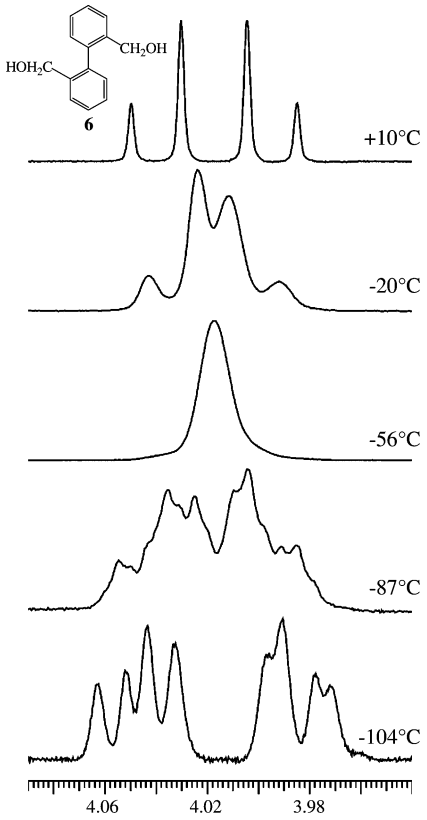

FIGURE 4. Temperature dependence of the ^{1}H signals (600 MHz) of the methylene hydrogens of **6** (ca. 0.07 M in CD$_2$Cl$_2$/CHF$_2$Cl 9:1 v/v). The trace at −104 °C depicts the ABX-type spectrum due to the diastereotopic methylene hydrogens (geminal J = −11.7 Hz) of the heterochiral dimer of **6** which also displays two different couplings with the OH hydrogen (J = 6.7 and 3.7 Hz).

SCHEME 2. DFT Computed Relative Energies (kcal mol−¹) for the Conformers of 6 and 7 (Dotted Lines Indicate Hydrogen Bonds)

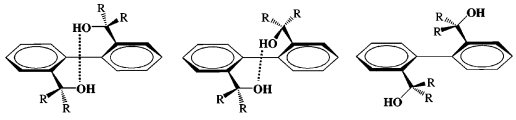

	(sp, sp)	(sp, ac)	(ap, ap)
R = H, **6**	E = 3.2	E = 0.0	E = 4.8
R= Me, **7**	E = 0.0	E = 3.8	E = 7.0

At ambient temperature, the amount of the dimer is conceivably quite small with respect to the monomer, and in any case, the exchange with the monomer is fast, so that only a four line AB spectrum can be observed (Figure 4, top trace). On lowering the temperature, the amount of the dimer increases progressively and, at the same time, the exchange rate diminishes, yielding spectra with lines broadened by the exchange.[14] At −87 °C, both superimposed spectra can be observed (see Figure S7 of the Supporting Information for spectral simulation) and at further low temperature (−104 °C) the monomer is totally absent; thus, only the spectrum of the dimer is observed.

(13) Meyer, W. L.; Meyer, R. B. *J. Am. Chem. Soc*. **1963**, *85*, 2171. Baitinger, W. F., Jr.; Schleyer, P. v. R.; Mislow, K. *J. Am. Chem. Soc*. **1965**, *87*, 3168.

In Figure 4 (bottom trace), the latter appears as an ABX-type spectrum, since at such low temperature the diastereotopic methylene hydrogens (having a geminal $J_{AB} = -11.6$ Hz) also display two different J couplings with the OH hydrogen ($J_{AX} = 6.7$ and $J_{BX} = 3.7$ Hz). Decoupling of the OH single broad line transforms, in fact, the eight-line ABX spectrum into a four-line AB spectrum. It should be also pointed out that when CD_3OD is used as solvent this process does not occur and only the four-line AB spectrum of the monomer is detected, even at very low temperature; in fact, the possibility for **6** of making a strong H-bond with this solvent makes formation of the dimer unlikely.[15]

The NMR spectral traces of **6**, however, are too complex[14] to allow a quantitative interpretation of the process, whereas derivative **7**, which yields simpler spectra, is better suited for obtaining a quantitative determination of the exchange dynamics.

In the latter derivative, the two ^{1}H lines of the diastereotopic methyl groups broaden on cooling, as observed in the spectrum of **6**, but in this case, two well-resolved spectra, due to two species with unequal populations, are observed at low temperature (33/67 in CD_2Cl_2/CHF_2Cl at − 115 °C, as in Figure 5). One such spectrum displays two equally intense lines (indicated as A in Figure 5); the other spectrum shows four equally intense integrated lines (indicated as B). The ratio of these two forms is greatly dependent on the type of solvent employed, up to the point of reversing their relative proportions, as summarized in Table 2.

The sp,sp conformer (which exhibits two equivalent CMe_2OH substituents) is by far the most stable form, according to DFT computations[7] (Scheme 2) and to X-ray data (see below) and should therefore be the only populated species (about 99%). Also in this case, the Ar−CMe_2OH rotation for interconverting the sp,sp into the second most stable sp,ac conformer is computed[7] to be only slightly higher (ca. 4 kcal mol^{-1}) than that of **6** and will likewise be invisible in the NMR, as experimentally found in the cases of the similar compounds **1**, **4**, and **5**. The two lines of the spectrum, indicated as A, should correspond to the diastereotopic methyl groups within the two equal CMe_2OH moieties of the most stable sp,sp conformer of Scheme 2, essentially in the monomeric situation. We again attributed the four line spectrum (labeled B) to a dimer, formed by two intermolecular H-bond interactions between the pairs of OH groups of two sp,sp conformers. DFT calculations[7] indicate that the energy of the homochiral dimer (M,M or P,P) is much lower than that of the heterochiral M,P (meso) dimer (Figure 6); thus, the latter should not be populated. In the most stable M,M (or in the isoenergetic P,P) chiral dimer, the eight methyl groups experience four different spatial environments[16] because there are two pairs of diastereotopic CMe_2OH moieties, each bearing two diastereotopic methyl groups. Four different shifts are, accordingly, expected for the methyl groups: since the homochiral dimer of **7** is racemic (C_2 static symmetry), even the rapid rotation about the C−OH bonds maintain diastereotopic the two pairs of CMe_2OH moieties, contrary to the case of the CH_2OH moieties of the meso dimer of **6**).

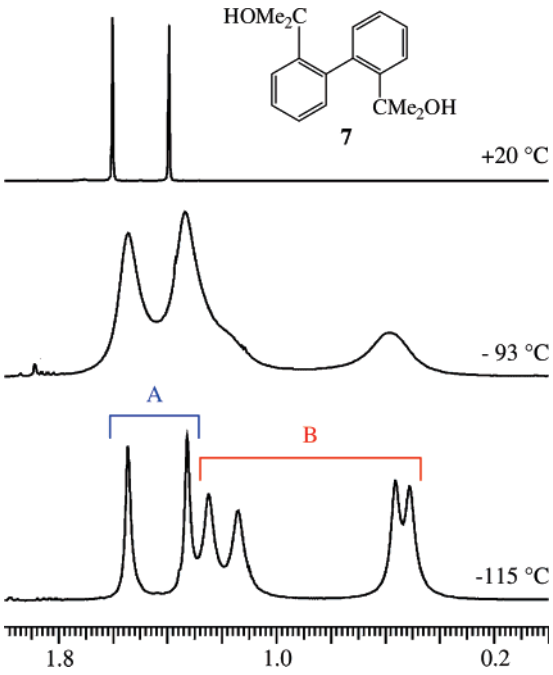

FIGURE 5. ^{1}H NMR signals (600 MHz in CD_2Cl_2/CHF_2Cl 9:1 v/v) of the diastereotopic methyl groups of **7** (top trace). On lowering the temperature these lines broaden (central trace), and at −115 °C (bottom trace) the spectrum displays two lines for the form A (33%) and four lines for the form B (67%).

TABLE 2. Relative Proportion (%) of the Two Spectral Traces of the Methyl Groups of 7 in Various Solvents at −115 °C

solvent	CD_2Cl_2[a]	toluene-d_8[a]	CD_3OD[a]	$CHFCl_2/CHF_2Cl$
two-line spectrum (A)	33	10	100	84
four-line spectrum (B)	67	90	0	16

[a] To lower the freezing point of the solutions a small amount of CHF_2Cl (∼10% v/v) was added.

(14) The complexity of the variable temperature spectra arises from the fact that in the range −20 to −60 °C the shift separation of the AB spectrum of the monomer changes and, furthermore, its lines are broadened by the exchange with an increasing amount of the dimer, until a single broad line is observed at −56 °C. In the range −60 to −85 °C, both the spectrum of the dimer and that of the monomer begin to appear as superimposed traces, with the widths of the lines still broadened by the exchange. At −87 °C, approximately 12 broad humps are observed, due to the four lines of the monomer superimposed to the eight lines of the dimer in a slow exchange regime: simulation of this spectrum (Figure S7, Supporting Information) indicates that the dimer/ monomer ratio is 88/12. Such an observation allowed us to rule out the possibility that the dynamic process is due solely to the mobility of the OH hydrogen (moving from one OH to another), because this motion alone cannot produce a spectrum with more than eight lines. Only below −100° C could a well-resolved spectrum be observed, since the only species present at this temperature is that of the dimer (Figure 4, bottom trace). In the latter, the coupling with the OH hydrogen could be detected because these hydrogens are not mobile: they are firmly bonded to the oxygen, because the OH groups are involved in the strong intermolecular hydrogen bonds required to form the dimer. In the monomer, on the contrary, the OH hydrogens, not involved in a strong hydrogen bond, are very mobile and can rapidly exchange among the various molecules, thus making such a coupling invisible (see: Jackman, L. M.; Sternhell, S. *Application of NMR Spectroscopy in Organic Chemistry*, 2nd ed.; Pergamon Press: Oxford, 1969; p 17).

(15) Ikeda, C.; Nagahara, N.; Motegi, E.; Yoshioka, N.; Inoue, H. *Chem. Comm*. **1999**, 1759. Escuder, B.; LLusar, M.; Travet, J. F. *J. Org. Chem*. **2006**, *71*, 7747.

(16) The four-line spectrum displays two lines at a field quite higher than the other two spectra (in CD_2Cl_2 the shifts are, respectively, 0.50, 0.55 and 1.13, 1.24 ppm). As evident from the computed structure of the M,M dimer (Figure 6), two pairs of methyl groups lie above the aryl rings and thus experience the well known upfield shift due to the aromatic ring current (see: Jackman, L. M.; Sternhell, S. *Application of NMR Spectroscopy in Organic Chemistry*, 2nd ed.; Pergamon Press: Oxford, 1969; p 95. Jennings, W. B.; Farrell, B. M.; Malone, J. F. *Acc. Chem. Res*. **2001**, *34*, 885. Wüthrich, K. *Angew. Chem. Int. Ed*. **2003**, *42*, 3340). The DFT-computed shifts for the MM dimer display an analogous trend, i.e., 1.51, 1.21 ppm for the two pairs of methyls at lower field and 1.16, 1.14 ppm for the two pairs of methyls at higher field, the latter actually corresponding to the methyls lying above the phenyl rings.

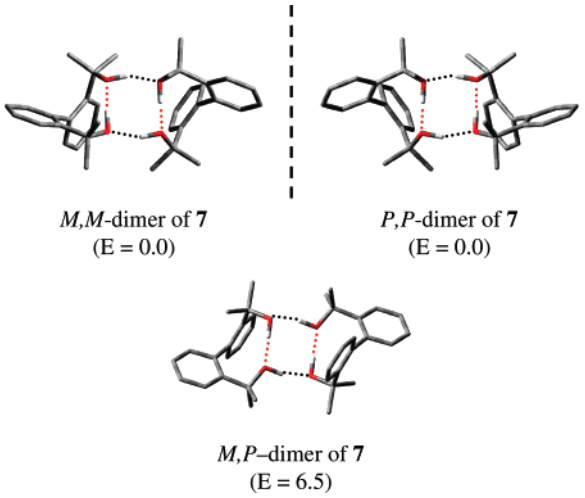

FIGURE 6. DFT-computed structures of the two possible dimers derived from the association between two enantiomers of the most stable conformer (sp,sp) of compound **7**. In the most stable chiral dimer (top), in addition to the two intramolecular hydrogen bonds (indicated by the red dotted lines), there are two intermolecular hydrogen bonds (indicated by two black dotted lines) connecting the two monomers. The relative minimum energy (*E*, kcal mol^{-1}) for the achiral (meso) dimer formed by the association of an M and of a P enantiomer (bottom) is much higher than that for the dimer due to the association of two M (or two P) enantiomers (top).

As previously mentioned, the amount of a dimer is conceivably quite small with respect to the monomer at higher temperatures and, since the exchange with the monomer is fast, only the two-line spectrum can be observed. On lowering the temperature, the amount of the dimer increases progressively as the rate of exchange diminishes. As a consequence, the lines begin to broaden and finally yield distinguishable spectra for the monomer and the dimer, the proportion of the latter growing, as conceivable, on further lowering the temperature (for instance, from 46% at −100 °C to 72% at −120 °C in CD_2Cl_2/CHF_2Cl).

The following experimental evidences seem to further support the hypothesis of a monomer/dimer equilibrium:

(i) When very diluted (less than 10^{-3} molar) solutions of **7** are examined, only the two line spectrum is invariably observed in any solvent at any low temperature. Under these conditions, in fact, the probability of forming a dimer has become negligible and only the spectrum of the monomer is therefore present (Figure S8, Supporting Information, reports some spectra obtained at −115 °C at various concentrations in CD_2Cl_2).

(ii) At any concentration in CD_3OD solutions only the two-line spectrum is observed, as reported for **6**. As mentioned, it is more likely that the H-bond takes place with methanol, thus preventing the occurrence of the H-bond between two molecules to produce the dimer.[15] Likewise, when a wholly fluorinated solvent is employed ($CHF_2Cl/CHFCl_2$) it is possible to have H-bonds between OH and fluorine.[17] This type of H-bond is weaker than in the case of methanol[18] and thus accounts for the quite small, although not negligible, proportion of the four-line spectrum observed in this solution (Table 2).

(iii) When the possibility of making a hydrogen bond with the solvent is negligible (as in the case of toluene and methylene chloride), the proportion of the dimer in toluene (Table 2), which has a small dielectric constant, is larger, at a given temperature, than in methylene chloride, which has a larger dielectric constant; this is in keeping with the computed value of the dipole moment of the M,M (or P,P) dimer (0.3 D) which is lower than that computed for the sp,sp monomer (2.3 D).

(iv) In the absence of exchange, the lines of the four-line spectrum B are broader than those of the two-line spectrum A (see the traces at −115 and −121 °C of Figures 5 and S8, Supporting Information, respectively). It is well-known that the line widths of molecules of larger dimensions are broader than those of smaller molecules, due to the longer correlation time,[19] this feature being particularly evident at very low temperatures. This agrees with the hypothesis that the four-line spectrum corresponds to a dimer which, obviously, has a larger dimension, thus broader lines, than the monomer.

(v) A diffusion ordered spectroscopy NMR (DOSY)[20] experiment was performed in a diluted (10^{-3} M) and in a concentrated (10^{-1} M) solution of **7** in toluene-d_8. In the latter solution a certain amount of dimer should be present at the equilibrium with the monomer, and indeed, a lower diffusion coefficient (8.7 ± 0.1 10−10 m^2 s^{-1}) was measured with respect to the diluted solution (9.6 ± 0.1 10^{-10} m^2 s^{-1}) where the dimer is absent. The hydrodynamic volume obtained for the concentrated (359 Å^3) was accordingly larger than for the diluted solution (272 Å^3), confirming the presence of a certain amount of a form with a larger molecular size.[21]

The process interconverting the two monomers into a dimer depends on the concentration, according to a second-order rate constant. As an example, the spectral simulation for a 0.13 M solution of **7** in $CHF_2Cl/CHFCl_2$ is displayed in Figure S9 (Supporting Information). From the lifetime (τ) values, a $\Delta G^{\ddagger}$ of 9.5 ± 0.3 kcal mol^{-1} was obtained in the temperature range −80 to −94 °C: to the best of our knowledge, this is the first example of a quantitative NMR determination of a dynamic process involving a monomer/dimer exchange.

Also compounds **8** and **9**, having ortho substituents R larger than those of **6**, yield spectra exhibiting, respectively, diastereotopic ethyl and isopropyl groups at ambient temperature. Contrary to the case of **6** and **7**, however, they do not display at low temperatures the signals attributable to the dimer, indicating that only the monomer is present. The larger dimensions of these compounds make it very difficult to realize the close approach of the OH groups of two molecules, as required to produce a sufficiently stable dimer. According to calculations, the most stable conformer in both **8** and **9** has the same type of sp,sp structure as that of the corresponding conformer of **7**, due to the presence of the intramolecular hydrogen bond.

X-ray Diffraction. The known[22] crystal structure of compound **6**, obtained on crystals grown from acetone, shows that

(17) Howard, J. A. K.; Hoy, V. J.; O'Hagan, D.; Smith, G. T. *Tetrahedron* **1996**, *52*, 12613. Alkorta, I.; Rozas, I.; Elguero, J. *J. Fluorine Chem.* **2000**, *101*, 233.

(18) The H-bond energy of a OH group with organofluorine compounds is estimated to be between 2.4 kcal mol^{-1} (Howard, J. A. K.; Hoy, W. J.; O'Hagan, D.; Smith, G. T. *Tetrahedron* 1**996**, *52*, 12613) and 3 kcal mol^{-1} (Bettinger, H. F. *Chem. Phys. Chem*. **2005**, *6*, 1169), to be compared with the 9 kcal mol^{-1} of the H-bond with methanol (Pimentel, G. C.; McClellan, A. L. *The Hydrogen Bond*; Freeman and Co.: San Francisco 1960; p 99).

(19) Claridge, T. D. W. *High Resolution NMR Techniques in Organic Chemistry*; Pergamon Press: Oxford 1999; p 36.

(20) Johnson, C. S., Jr. *Prog. Nucl. Magn. Reson. Spectrosc*. **1999**, *34*, 203. Cohen, Y.; Avram, L.; Frish, L. *Angew. Chem., Int. Ed*. **2005**, *44*, 520. Pregosin, P. S.; Kumar, P. G. A.; Fernandez, I. *Chem. Rev*. **2005**, *105*, 2977. Dehner, A.; Kessler, H. *ChemBioChem* **2005**, *6*, 1550.

(21) Cabrita, E. J.; Berger, S. *Magn. Reson. Chem.* **2001**, *39*, 3142. Valentini, M.; Rüegger, H.; Pregosin, P. S. *Helv. Chim. Acta* **2001**, *84*, 2833.

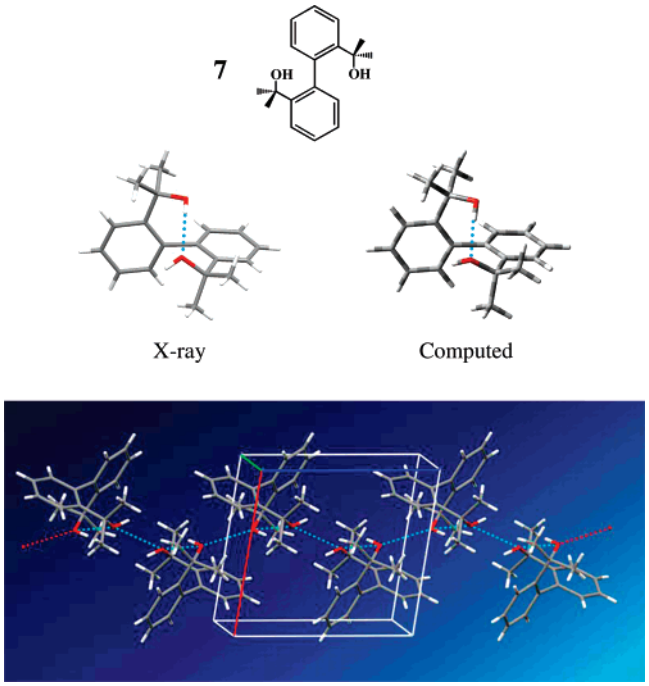

FIGURE 7. Top: X-ray structure (left) and DFT-computed structure (right) of compound **7**. Bottom: crystallographic cell showing the presence of both intra- and intermolecular H-bond (dotted cyan lines).

the molecule exists essentially as a dimer formed by a pair of heterochiral molecules kept together by a H-bond; the dimers are then linked together to form a supramolecular chain. To avoid the possibility of polymorphism induced by the solvent, we also obtained crystals from a very low polarity solvent (hexane). Our crystal structure is exactly equal to the reported one (see the Supporting Information, Figure S6). Such an experimental result thus confirms the theoretical computations and also agrees with the interpretation of the NMR spectra in solution. There is a slight deviation in the shape of the preferred conformer in the solid state as compared to that computed for the isolated molecule, this being a consequence of the lattice interactions experienced by the dimer in the crystalline state.

The crystal structure of **7** (Figure 7) confirms the presence of an extended network of H-bonds; however, at variance with **6**, the sp,sp conformation of the molecule of **7** in the solids indicates the presence of an intramolecular H-bond and an intermolecular H-bond with another molecule of opposite chirality. This arrangement should correspond to a weaker intermolecular interaction with respect to the case of **6**, in which each molecule has two intermolecular H-bond. This agrees with the fact that in solution we were able to observe distinguishable NMR spectra for the monomer and the dimer of **7** at low temperature, whereas in the case of **6** only the spectrum of the dimer was present at low temperature.

The single-crystal X-ray structure of compound **9** does show the presence of the intramolecular H-bond, but it does not show

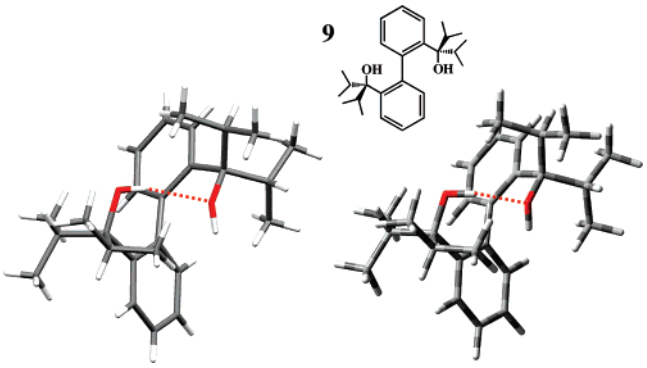

FIGURE 8. Single crystal X-ray structure (left) of compound **9** and DFT computed structure (right) of its most stable conformer (sp,sp).

the existence of any intermolecular H-bond, thus preventing the formation of a dimer, a feature in good agreement with the result of the NMR spectra.[23] In addition, the sp,sp conformation predicted by the theory turns out to be very close to that found by X-ray diffraction (Figure 8).

Circular Dicroism and Absolute Configuration. In all derivatives bearing two equal CR_2OH substituents (**6**−**9**), the high Ar−Ar rotation barrier entails the lack of a plane or center of symmetry, thus leading to M and P enantiomers, which can be made visible by taking the NMR spectrum in a chiral environment[24] (for instance, the bottom trace of Figure S10, Supporting Information, displays four methyl lines, i.e., a pair of lines for each of the two diastereotopic methyl groups of **7**).

The observation that the NMR lines of the R groups appear anisochronous at any attainable high temperature agrees with the results of calculations[7] predicting very high enantiomerization barriers (for instance, 38.2 kcal mol^{-1} in the case of **7**). This implies that these types of atropisomers are configurationally stable, and indeed we were able to achieve a physical separation in the case of **7** by means of the enantioselective HPLC technique (Experimental Section): the corresponding circular dicroism (CD) spectra display the expected opposite phased traces (Figure S11, Supporting Information).

The experimental CD and absorption spectra of the first eluted enantiomer of **7** are reported in Figure 9. The absorption spectrum shows a weak ($\epsilon \approx 200$) band centered around 265 nm, a clear shoulder 220 nm (with $\epsilon \approx 12000$) followed by a monotonic increase of the absorption down to 200 nm where $\epsilon \approx 40000$. These data are typical of a benzene chromophore[25] and very different from those of a conjugated biphenyl chromophore. This confirms that in compound **7** the two benzene rings are completely nonconjugated or, in other words, the dihedral angle defined by the two aromatic planes is of the order of 90°, in full agreement with the previous analysis based on the NMR behavior. The CD spectrum shows very weak bands (of both the signs) in the range 280−250 nm, a weak positive ($\Delta\epsilon$ +0.15) band at 240 nm, followed by two Cotton effects at 222 nm ($\Delta\epsilon$ −7.8) and at 200 nm ($\Delta\epsilon$ +11), respectively.

In order to deduce the absolute configuration (AC) of the first eluted enantiomer of **7** we simulated by theoretical methods

(22) Rajnikant, Dinesh.; Sharma, B.; Singh, D. *J. Chem. Crystallogr.* **2006**, *36*, 331.

(23) In derivative **9**, the two isopropyl moieties are diastereotopic because of the chirality of the molecule (due to the highly hindered Ar-Ar rotation), so that the ^1H and ^{13}C signals of the corresponding CH moieties are anisochronous even at ambient temperature. Since these lines are already split, it is not possible to observe the splitting due to the restricted rotation of the isopropyl groups at low temperature, as it had been done in the case of **3** (Figure 3).

(24) Use was made of a 11:1 molar excess of the enantiopure (*R*)-(−)-2,2,2-trifluoro-1-(9-anthryl)ethanol (Pirkle, W. H.; Sikkenga, D. L.; Pavlin, M. S. *J. Org. Chem.* **1977**, *42*, 384).

(25) (a) Jaffè, H. H.; Orchin, M. *The Theory and Application of UV Spectroscopy;* J. Wiley and Sons: New York, 1962. (b) Suzuki, H. *Electronic Absorption Spectra and Geometry of Organic Molecules*; Academic Press: New York, 1967.

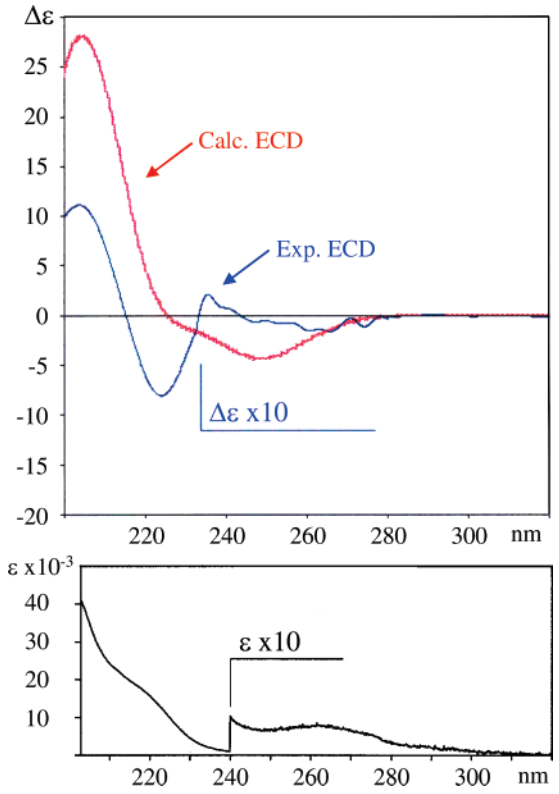

FIGURE 9. Absorption (lower trace, black) and experimental CD (upper trace, blue) spectra in acetonitrile of the first eluted enantiomer of **7**. The red trace is the computed one (see text).

the experimental CD spectrum, assuming arbitrarily one of the two absolute configurations, and compared the predicted result with that of the experiment. If the shape of the theoretical spectrum is comparable with the experimental one, the assumed AC should correspond to the true configuration: on the contrary, if the data are in an almost mirror image relationship, the true molecular AC is opposite to that assumed for the calculations. Toward this goal, use was made of the TD-DFT/B3LYP method (implemented in the Gaussian 03 program[7]), since such a technique has been employed successfully several times[26] to simulate ECD spectra. The geometries of the three structures had been already optimized at the B3LYP/6-31G(d) level, leading to the relative energies reported in Scheme 2.[27] Since, as previously mentioned, the most stable sp,sp conformer of **7** should be 99% populated (this structure was also confirmed by X-ray diffraction as in Figure 7), all of the ECD calculations have been carried out solely for this structure. The transitions energies, oscillator strengths, and rotational strengths of the absolute configuration P for the lowest 20 states are collected in Table S1 (Supporting Information). The oscillator strengths are plotted in Figure S12 (Supporting Information) with the experimental UV spectrum.

Reasonably, the experimental band observed at 262 nm can be assigned to the excitation 1, while the intense absorption beginning at ~240 nm, and measured down to 200 nm, can be assigned to the group of excitations 5−10. Rotational strengths of the same 20 states have been calculated using both the length and velocity representations. It is clear that the results obtained using the two different formalisms[26] are actually very similar: this indicates the high quality of the calculations. The velocity rotational strengths are plotted in the Figure S13 (Supporting Information), together with the theoretical CD spectrum obtained[26k,l] from these values, using a Gaussian band shape (σ 0.15 eV). The theoretical CD spectrum (red trace) for the P configuration of **7** is compared to the experimental spectrum (blue trace) in Figure 9.

The positions of the CD intensity maxima in the theoretical spectrum do not perfectly match those of the experimental spectrum and the predicted ECD intensities are in general larger than the experimental data. Nevertheless, the experimental spectrum shows a sequence of very weak negative, positive bands followed by a much stronger negative Cotton effect followed, in turn, by a positive CD band at about 205 nm. The same features are reproduced in the theoretical spectrum, in particular the sequence of the most intense negative/positive Cotton effects (we could not record a further negative CD band predicted below 200 nm). In conclusion, it is quite safe to state that the first eluted enantiomer of **7** possesses the absolute configuration P and thus the second eluted has the configuration M, as shown in Figure S11 (Supporting information).

Conclusions

Biphenyl derivatives bearing a single CR_2OH substituent in the ortho position exist as sp and ap conformers due to the restricted rotation about the Ar-CR_2OH bond. Introduction of the prochiral *i*-Pr group in the position 3′ allowed the determination of the enantiomerization barrier due to the Ar−Ar bond rotation. DFT computations of the barriers and of the relative stability of the two conformational isomers were all in agreement with the experiments.

Biphenyls bearing two CR_2OH groups in the 2,2′ positions were found to exist as configurationally stable enantiomers: when R = Me (**7**) they were separated by enantioselective HPLC and the absolute configuration assigned on the basis of the corresponding CD spectra.

(26) For TDDFT-CD calculations, see: (a) Diedrich, C.; Grimme, S. *J. Phys. Chem. A* **2003**, *107*, 2524. (b) Autschbach, J.; Ziegler, T.; van Gisbergen, S. J. A.; Baerends, E. J. *J. Chem. Phys.* **2002**, *116*, 6930. (c) Pecul, M.; Ruud, K.; Helgaker, T. *Chem. Phys. Lett.* **2004**, *388*, 110. (d) Grimme, S.; Bahlmann, A. *Modern Cyclophane Chemistry* **2004**, 311. (e) Braun, M.; Hohmann, A.; Rahematpura, J.; Buehne, C.; Grimme, S. *Chem. Eur. J.* **2004**, *10*, 4584. (f) Furche, F.; Ahlrichs, R.; Wachsmann, C.; Weber, E.; Sobanski, A.; Voegtle, F.; Grimme, S. *J. Am. Chem. Soc.* **2000**, *122*, 1717. (g) Stephens, P. J.; McCann, D. M.; Butkus, E.; Stoncius, S.; Cheeseman, J. R.; Frisch, M. J. *J. Org. Chem.* **2004**, *69*, 1948. (h) Stephens, P. J.; McCann, D. M.; Devlin, F. J.; Cheeseman, J. R.; Frisch, M. J. *J. Am. Chem. Soc.* **2004**, *126*, 7514. (i) Neugebauer, J.; Baerends, E. J.; Nooijen, M.; Autschbach, J. *J. Chem. Phys.* **2005**, *122*, 234305/1−234305/7. (j) Pecul, M.; Marchesan, D.; Ruud, K.; Coriani, S. *J. Chem. Phys.* **2005**, *122*, 024106/1−024106/9. (k) Giorgio, E.; Tanaka, K.; Ding, W.; Krishnamurthy, G.; Pitts, K.; Ellestad, G. A.; Rosini, C.; Berova, N. *Bioorg. Med. Chem.* **2005**, *13*, 5072. (l) Mori, T.; Inoue, Y.; Grimme, S. *J. Org. Chem.* **2006**, *71*, 9797. (m) Stephens, P. J.; McCann, D. M.; Devlin, F. J.; Smith, A. B., III. *J. Nat. Prod.* **2006**, *69*, 1055. (n) Stephens, P. J.; Pan, J.-J.; Devlin, F. J.; Urbanova, M.; Hajicek, J. *J. Org. Chem.* **2007**, *72*, 2508.

(27) We decided also to use the MM approach to reduce the computational effort, considering the size of molecule. Therefore, the starting geometries have been created by means of a conformational analysis with the SPARTAN02 software, using the methods of molecular mechanics (MMFF94s force field) and retaining all the structures differing by 2 kcal/mole in energy or less. Assuming P as absolute configuration, three stable conformers have been found in the gas phase: their structures are of the same type shown in Scheme 2 (in this approximate approach the populations are however different with respect to the DFT computations being 89.2%, 7,4% and 3.4 % for the sp,sp, sp,ac, and ap,ap, respectively). The most stable conformer is characterized by a dihedral angle θ between the aromatic rings of about 90°, by intermolecular hydrogen bond between the two −OH groups and by the fact that the two methyl groups are placed far away, reducing completely the steric repulsions.

Compounds **6** (R = H) and **7** (R= Me) were found to exist as dimers in solution, due to intermolecolar H-bond interactions. In the case of **7**, the free energy of activation (9.5 kcal mol^{-1}) for the exchange of the monomers with the dimer could be measured by dynamic NMR. The conformational preferences, predicted by computations, were confirmed by X-ray diffraction in the case of R = H (**6**), R = Me (**7**), and R = *i*-Pr (**9**).

Experimental Section

Materials. 2,2′-Dibromobiphenyl[28] was prepared according to the literature. 2-Bromobiphenyl and 2,2′-biphenyldimethanol (**6**) were commercially available. Compound **6** was further purified by semipreparative HPLC on a C18 column (5 μm, 250 × 10 mm, 5 mL/min, ACN/H_2O 90:10 v/v); crystals suitable for X-ray diffraction were obtained from hexane.

General Procedure for 1−3. A solution of 2-lithium biphenyl was prepared in 1 h by addition of 6.3 mL of *n*-butyllithium (10 mmol, 1.6 M in hexane) to a stirred solution of 1.08 g of 2-bromobiphenyl (10 mmol in 40 mL of anhydrous THF) kept at −78 °C. To the solution was then slowly added a solution of the appropriate ketone (acetone, diethylketone, diisopropyl ketone, 8 mmol in 30 mL of anhydrous THF). After 1 h at −78 °C, the mixture was warmed to ambient temperature and quenched with aqueous NH_4Cl. The extracted organic layer (Et_2O) was dried (Na_2SO_4) and evaporated, and the crude was purified by chromatography on silica gel (hexane/Et_2O 10:1) to obtain compounds **1−3**. Analytically pure samples were obtained by semipreparative HPLC on a C18 column (5 μm, 250 × 10 mm, 5 mL/min, ACN/H_2O 70:30 v/v or 80:20 v/v). See the Supporting Information for spectroscopic data.

2-(3′-Isopropylbiphenyl-2-yl)propan-2-ol (4). A solution of Me-Li (5 mmol, 1.5 M in Et_2O) was slowly added to a solution of 1-(3′-isopropylbiphenyl-2-yl)ethanone[29] (2 mmol in THF), kept at −78 °C. After 1 h at −78 °C, the mixture was warmed to ambient temperature and quenched with aqueous NH_4Cl. The extracted organic layer (Et_2O) was dried (Na_2SO_4) and evaporated, and the crude was purified by chromatography on silica gel (hexane/Et_2O 10:1) to obtain compound **4**. Analytically pure samples were obtained by semipreparative HPLC on a C18 column (5 μm, 250 × 10 mm, 5 mL/min, ACN/H_2O 80:20 v/v). See the Supporting Information for spectroscopic data.

2-(2′-Methylbiphenyl-2-yl)propan-2-ol (5). A solution of (2′-bromobiphenyl-2-yl)lithium was prepared in 1 h by addition of 6.5 mL of *n*-butyllithium (10,4 mmol, 1.6 M in hexane) to a stirred solution of 3.12 g of 2,2′-dibromobiphenyl (10 mmol in 40 mL of anhydrous THF) kept at −78 °C. To this solution was then slowly added a solution of Me-I (2.84 g, 20 mmol in 10 mL of anhydrous THF). After 1 h at −78 °C, the mixture was warmed to ambient temperature and quenched with aqueous NH_4Cl. The formation of 2-bromo-2′-methylbiphenyl was checked by GC−MS (*m*/*z* 246). The extracted organic layer (Et_2O) was then dried (Na_2SO_4) and evaporated. To a cooled (−78 °C) solution of the crude (2.2 g, about 9 mmol in 40 mL of THF) were then added 6.5 mL of *n*-butyllithium (10.4 mmol, 1.6 M in hexane) and, after 1 h, a solution of acetone (1.16 g, 20 mmol in 5 mL of THF). After 1 h at −78 °C, the mixture was warmed to ambient temperature and quenched with aqueous NH_4Cl. The extracted organic layer (Et_2O) was dried (Na_2SO_4) and evaporated, and the crude was purified by chromatography on silica gel (hexane/Et_2O 10:1) to obtain compound **5**. Analytically pure samples were obtained by semipreparative HPLC on a C18 column (5 μm, 250 × 10 mm, 5 mL/min, ACN/H_2O 80:20 v/v). See the Supporting Information for spectroscopic data.

General Procedure for 7−9. A solution of the 2,2′-dilithiobiphenyl was prepared in 1 h by addition of 14.0 mL of *n*-butyllithium (22,4 mmol, 1.6 M in hexane) to a stirred solution of 3.12 g of 2,2′-dibromobiphenyl. (10 mmol in 40 mL of anhydrous THF) kept at −78 °C. To this solution was then slowly added a solution of the appropriate electrophile (acetone, diethylketone, or diisopropyl ketone, 30 mmol in 10 mL of anhydrous THF). After 1 h at −78 °C, the mixture was warmed to ambient temperature and quenched with aqueous NH_4Cl. The extracted organic layer (Et_2O) was dried (Na_2SO_4) and evaporated, and the crude was purified by chromatography on silica gel (hexane/Et_2O 10:1) to obtain compounds **7−9**. Analytically pure samples were obtained by semipreparative HPLC on a C18 column (5 μm, 250 × 10 mm, 5 mL/min, ACN/H_2O 80:20 v/v or 90:10 v/v). Crystals suitable for X-ray diffraction were obtained by slow evaporation in the case of **7** (from toluene) and **9** (from acetonitrile). See the Supporting Information for spectroscopic and crystallographic data.

NMR Spectroscopy. The spectra were recorded at 400 and 600 MHz for ^1H and 100.6 and 150.8 MHz for ^{13}C. The assignments of the ^{13}C signals were obtained by bidimensional experiments (edited-gHSQC[30] and gHMBC[31] sequences). The samples for obtaining spectra at temperatures lower than −100 °C were prepared by connecting to a vacuum line the NMR tubes containing the compound and a small amount of C_6D_6 (for locking purpose) and condensing therein the gaseous CHF_2Cl and $CHFCl_2$ (4:1 v/v) under cooling with liquid nitrogen. The tubes were subsequently sealed in vacuo and introduced into the precooled probe of the spectrometer. The temperatures were calibrated by substituting the sample with a Cu/Ni thermocouple before the measurements. Low temperature ^{13}C spectra were acquired with a 5 mm dual probe, without spinning, with a sweep width of 38000 Hz, a pulse width of 4.9 μs (70° tip angle), and a delay time of 2.0 s. Proton decoupling was achieved with the standard Waltz-16 sequence. A line broadening function of 1−5 Hz was applied to the FIDs before Fourier transformation. Usually 512−1024 scans were acquired. The line shape simulations were performed by means of a PC version of the QCPE program DNMR 6 no. 633, Indiana University, Bloomington, IN. The NOE experiments were obtained by means of the DPFGSE-NOE[32] sequence. To selectively irradiate the desired signal, a 50 Hz wide shaped pulse was calculated with a refocusing-SNOB shape[33] and a pulse width of 37 ms. DOSY experiments were obtained in toluene-d_8 at +22 °C by means of the BPLED pulse sequence[34] with a delay diffusion of 0.020 and 0.025 s. Gradient strength was varied from 0.4 to 66 g/cm. Gradient calibration was obtained on a HDO/D_2O sample, for which the diffusion coefficient was known[35] (19.2×10^{-10} m^2 s^{-1}). The diffusion coefficient *D* was obtained from the Stejskal-Tanner equation, and the hydrodynamic radius was evaluated by the Stokes−Einstein equation, using a viscosity value for toluene[36] equal to 0.575 mPa·s.

Calculations. Computations were carried out at the B3LYP/6-31G(d) level by means of the Gaussian 03 series of programs[7] (see

(28) Gilman, H.; Gorsich, R. D. *J. Am. Chem. Soc.* **1956**, *78*, 2217.
(29) Lunazzi, L.; Mazzanti, A.; Minzoni, M. *J. Org. Chem.* **2006**, *71*, 9297.
(30) Bradley, S. A.; Krishnamurthy, K. *Magn. Reson. Chem.* **2005**, *43*, 117. Willker, W.; Leibfritz, D.; Kerssebaum, R.; Bermel, W. *Magn. Reson. Chem.* **1993**, *31*, 287.
(31) Hurd, R. E.; John, B. K. *J. Magn. Reson.* **1991**, *91*, 648.
(32) (a) Stott, K.; Stonehouse, J.; Keeler, J.; Hwand, T.-L.; Shaka, A. J. *J. Am. Chem. Soc.* **1995**, *117*, 4199. (b) Stott, K.; Keeler, J.; Van, Q. N.; Shaka, A. J. *J. Magn. Reson.* **1997**, *125*, 302. (c) Van, Q. N.; Smith, E. M.; Shaka, A. J. *J. Magn. Reson.* **1999**, *141*, 191. (d) See also: Claridge, T. D. W. *High Resolution NMR Techniques in Organic Chemistry*; Pergamon: Amsterdam 1999.
(33) Kupče, E.; Boyd, J.; Campbell, I. D. *J. Magn. Reson. Ser. B* **1995**, *106*, 300.
(34) Wu, D.; Chen, A.; Johnson, C. S. *J. Magn. Reson. A* **1995**, *115*, 260.
(35) Tyrrell, H.J. W; Harris, K.R. *Diffusion in Liquids*; Butterworth: London, 1984.
(36) Santos, F. J. V.; Nieto de Castro, C. A.; Dymond, J. H.; Dalaouti, N. K.; Assale, M. J.; Akira Nagashima, A. *J. Phys. Chem. Ref. Data* **2006**, *35*, 1.

the Supporting Information): the standard Berny algorithm in redundant internal coordinates and default criteria of convergence were employed. The reported energy values are not ZPE corrected. Harmonic vibrational frequencies were calculated for all the stationary points. For each optimized ground state the frequency analysis showed the absence of imaginary frequencies, whereas each transition state showed a single imaginary frequency. Visual inspection of the corresponding normal mode was used to confirm that the correct transition state had been found. NMR chemical shift calculation were obtained with the GIAO method at the Pw1Pw91/6-311+G(2d,p)//B3LYP/6-31G(d) level. TMS, calculated at the same level of theory, was used as reference to scale the absolute shielding value.

Acknowledgment. Thanks are due to Dr. C. Coluccini, University of Bologna, Italy, for assistance during the synthesis of some compounds. L.L. and A.M. received financial support from the University of Bologna (funds for selected research topics and RFO) and from MIUR-COFIN 2005, Rome (national project "Stereoselection in Organic Synthesis").

Supporting Information Available: DFT-computed structure for **1**−**3** (Figure S1); NOE spectra of **1** (Figure S2); VT NMR of the ^{13}C CH_2 signals of **2** (Figure S3); VT NMR of the ^{1}H CH signal of **3** (Figure S4); VT NMR of the methyl signals of **5** (Figure S5); DFT-computed and X-ray structure of **6** (Figure S6); NMR simulation of compound **6** (Figure S7); spectra of the ^{1}H methyl region of compound **7** at different concentrations (Figure S8); VT NMR of the ^{1}H methyl signal of **7** (Figure S9); spectra of **7** obtained in chiral medium (Figure S10); enantioselective HPLC trace and CD spectra of the enantiomers of compound 7 (Figure S11); comparison of the computed oscillator strengths of the absolute configuration P to the experimental absorption spectrum of compound **7** (Figure S12); computed velocity rotational strengths and CD spectrum for the absolute configuration P of compound **7** (Figure S13); DFT-calculated excitation energies, oscillator, and rotational strengths for the P configuration of compound **7** (Table S1); spectroscopic data for **1**−**5** and **7**−**9**; crystallographic data for compounds **6**, **7**, and **9**; ^{1}H and ^{13}C NMR spectra of **1**−**9**; HPLC analytical traces of **1**−**9**; chemical shift calculation for compound **3**; computational details of **1**−**9**. This material is available free of charge via the Internet at http://pubs.acs.org.

JO701481M